

## Photovoltaic Module Thermal Regulation: Effect of the Cells Arrangement Configurations on the Performance

Ahmed Hamza H. Ali<sup>a</sup>, Y. Matsushita<sup>a</sup>, S. Ookawara<sup>b</sup>

<sup>a</sup> Department of Energy Resources and Environmental Engineering, Egypt-Japan University of Science and Technology (E-JUST), P.O. Box 179, New Borg El-Arab City, Alexandria 21934, Egypt

<sup>b</sup> Department of Chemical Engineering, Tokyo Institute of Technology, Tokyo 1528551, Japan

---

### Abstract

This study is carried out to clarify experimentally the effect of higher PV module temperature on the module output power when the module works with and without thermal regulation system. Moreover theoretical study results are used to clarify which of the three configurations, in-line, oblique and offset of the cell location inside the channel, provide higher heat transfer rate at minimum friction factor. The results clearly indicate that, from the outdoor experimental measurements on PV module, the cell temperature is the prevailing parameter affecting the module output power more than the solar irradiance. While, based on the minimum friction factor for each configuration, the In-line plate segments configuration at certain design conditions provide the minimum friction factor, consequently, the minimum required pumping power, that will followed by higher PV module performance. Moreover, using PV modules in hot arid areas without thermal regulation leads to an increase in the total module areas ranging from 2.12 to 1.8 times that of module using thermal regulation system producing the same power.

**Keywords:** Photovoltaic-Thermal regulation (PV/T); In-line configuration; Offset plates; and Oblique plate segments

---

### 1. Introduction

The major applications of solar energy utilization are include solar thermal and solar photovoltaic (PV) systems. Photovoltaic (PV) modules convert a part of solar radiation energy directly into electricity, while, the unconverted part of the solar radiation into electricity is absorbed in a PV module leading it to experience very high temperatures. Commercially available PV modules have module label ratings and operating parameters based on the American Society for Testing Materials (ASTM) standard reporting conditions (SRC). The SRC are: solar irradiance  $GT = 1000 \text{ W/m}^2$ , cell temperature  $T_{\text{cell}} = 25^\circ\text{C}$ , and  $AM = 1.5$ . Thus, a typical 75 Watt PV module has 75 Watt label ratings at SRC. Ali [1] cited that, at  $30^\circ\text{C}$  ambient temperature with  $GT = 1000 \text{ W/m}^2$  and calm wind conditions a PV module reached a stagnation temperature of  $147^\circ\text{C}$  when it operated under open-circuit condition, and its temperature became  $135^\circ\text{C}$  when operated at the maximum power point. Moreover, it is cited in [1] that, increased PV

modules temperatures lead to decrease in its efficiency by 0.05% points per degree C rise relative to that value reported at SRC. Higher module temperature is followed by decrease in the output power, and in addition, it influences module lifetimes well as leads to degradation of the cell-wires junction function and encapsulation.

In hot arid reclaimed areas, the ambient temperature in the summer times exceeds  $45^\circ\text{C}$ , however it is expected that the PV modules temperature will be higher than  $135^\circ\text{C}$  when it works at maximum power point. Two main systems can be used for PV modules thermal regulation. They are classified based on the heat transfer fluid medium. One is water system, while the other is air system. Throughout the literature survey, PV modules thermal regulation systems are in research forms and are implemented mainly to increase the overall efficiency of PV/T systems, which produce both electric power and hot fluid particularly in northern climates. In hot arid reclaimed areas, water resources are scarce as well as the water systems need periodical maintenance, which is not easy to provide. In such circumstances, the photovoltaic modules thermal regulation is

---

\* Corresponding author. Tel.: +20 12 3971265

Fax: +20 3 459 9520; E-mail: [ahmed.hamza@ejust.edu.eg](mailto:ahmed.hamza@ejust.edu.eg)

© 2010 International Association for Sharing Knowledge and Sustainability

DOI: 10.5383/ijtee.02.01.006

preferred to be carried out using the air as the heat transfer fluid. The air duct flow system used for PV/T system in northern climate provides reasonable photovoltaic temperature due to moderate ambient temperature. However, for hot arid areas, the photovoltaic modules thermal regulation is preferred to be carried out using the air as the heat transfer fluid. The air at atmospheric conditions, normally, has low thermal and hydrodynamic properties. This limits its use in such system without significant change on conventional PV modules arrangement configuration. The PV modules are normally constructed from a number of solar cells wired in parallel and/or in series and fixed on rigid non-metallic flat plate. The upper surface facing the sun is covered with a material of high transmittance.

It is well known that the entrance region of a fluid flow in a heated duct or between two parallel plates channel is characterized by differentiates thermal and hydrodynamics boundary layers behaviors. In this case, the convective heat transfer coefficient is substantially larger than that at locations further downstream. Thus, using the flow interruption techniques in form of online segments, offset, or oblique plates in a duct, or a channel, to prevent fully developed flow formation has the advantage of obtaining enhanced heat-transfer characteristics. The flow interruption by leading edge applications were extended to air heater solar collectors, and, or a combined photovoltaic and air heater solar collector systems. One of the arrangements to utilize the leading edge effect and to prevent a fully developed flow, to enhance the convective heat transfer process, is by placing the segments inside a channel to form an in-line configuration as reported by Ali [1], while in form of oblique plates to flow is reported in Ali et al [2]. Also, offset configuration was used as presented by Ali [3], and Ali et al. [4]. For such in-line, oblique and offset configurations, the edge effect improves the heat transfer rate from both the upper and lower surfaces of the plate segments in a positive way but its not yet clarified which of these three configurations provide the highest heat transfer rate at minimum friction factor (pumping power) when the flow in the channel is laminar flow. Thus, for the air as a heat transfer fluid and flows within laminar flow regime through the three investigated configurations inside the channel, it is found that enhancement in the convective heat transfer processes occurred, while, clarification of which configuration can provide higher heat transfer rate at minimum friction factor need to be clarified. This study aims to clarify experimentally the effect of higher PV module temperature on the module output power when the module works with and without thermal regulation system. Moreover theoretical results are used to clarify which of the three configurations, in-line, oblique and offset of the cell location inside the channel, provide higher heat transfer rate at minimum friction factor.

## 2. Characteristic of Photovoltaic Module

The photovoltaic module characteristic parameters are the output power, which is obtained from multiplication of the DC Current (I) expressed in Ampere and Voltage (V) expressed in Volt. These parameters values are dependent on both the PV module temperature and incident solar irradiance. Module manufacturers commonly provide specification sheets at SRC having data values for four characteristic parameters, which are  $I_{sc}$ ,  $V_{oc}$ ,  $I_{mp}$ , and  $V_{mp}$ , where, the subscripts sc, oc, and mp stand for short circuit, open circuit and maximum output power respectively. In order to investigate the effect of suggested configuration on PV module characteristic parameters, the developed equations by Fitzpatrick [5], which predict the

effects of both temperature and solar irradiance on PV module characteristic are used. These equations are given as follows:

$$V_{mp}(T) = V_{mp}(T_r) - \beta_{V_{mp}} \cdot V_{mp}^{SRC} \cdot (T_r - T) \quad (1)$$

$$I_{mp}(T, G_T) = I_{mp}(T_r, G_{T_r}) \cdot \left(\frac{G_T}{G_{T_r}}\right) \cdot [1 - \alpha_{I_{mp}}(T_r - T)] \quad (2)$$

Equations (1) and (2) are used to determine the module maximum power characteristic parameters at any module temperature T and solar irradiance  $G_T$  from any known reference parameters temperature ( $T_r$ ) and solar irradiance ( $G_{T_r}$ ). The  $V_{mp}^{SRC}$  is the module maximum power voltage value at SRC, it is normally provided by the manufacturer. The coefficients  $\alpha_{I_{mp}}$  and  $\beta_{V_{mp}}$  in the equations are dimensioned by (1/C) and their typical values for some commercially available PV modules were cited in [5]. To best knowledge of the author the local market in Egypt has three firms producing the PV modules; none of them produces modules with thermal regulation system. To identify the effect of a PV module temperature on its output maximum power, outdoor measurement on one of the above mentioned firms PV modules is carried out to investigate its characteristics under actual operating condition different from the data at SRC. Therefore, measurements of  $I_{mp}$  and  $V_{mp}$  on labeled 75 W rated power (at SRC) single silicon crystal PV module is performed at the roof of the heat transfer laboratory at Assiut University, Egypt. This module was made from 36 series-connected solar cells embedded on a sheet of ethylene-vinyl-acetate and packed by multi-layer plastic foil sheets, while its front was covered with transparent glass cover. The PV module during measurements is loaded with both 62 W thermoelectric cooler and rechargeable battery to guarantee extraction of maximum possible output power.

## 3. Cells Arrangement Configurations

### 3.1 In-Line Plate Segments Configuration

A schematic diagram, for the configuration of the in-line plate segments inside the channel and dimensions are shown in Fig. 1, details of this configuration are presented in Ali [1]. Set of plates were used to form the in-line plate segments configuration as shown in Fig. 1. In this configuration, a distance between any two successive plate segments is located as a ratio form the plate length.

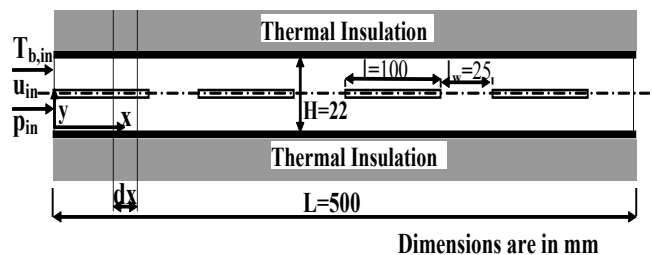


Fig. 1 A schematic diagram for the configuration of the in-line plate segments inside the channel

### 3.2 Oblique Plate Segments Configuration

A schematic diagram, for the configuration of plate segments tilted by angle ( $\gamma$ ) to the main flow direction in the X-axis is shown in figure (2) clarifying the module configuration. Details of this configuration are presented in Ali et al. [2]. In this configuration, a distance between any two successive plate segments is located as a ratio form the plate length.

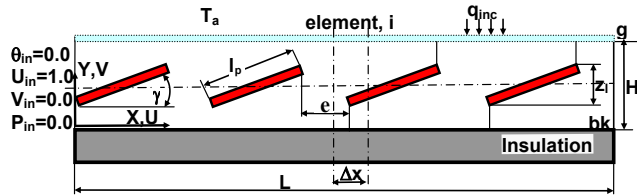


Fig. 2 A schematic diagram for the oblique plates configuration inside the channel

### 3.3 Offset Plate Segments Configuration

A schematic diagram, for the configuration of offset plate segments is shown in figure (2) clarifying the module configuration. Details of this configuration are presented in Ali [3]. In this configuration, a distance between any two successive plate segments is set zero, while the plates' location inside the flow channel is a ratio from the channel height.

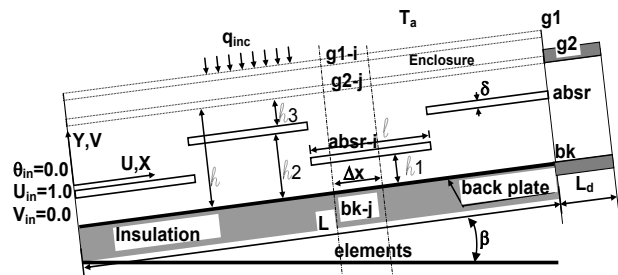


Fig. 3 A schematic diagram for the offset plates configuration inside the channel

### 3.4 Analysis

Details of the model developed that describes viscous flow and the flow field temperature boundary condition within the geometry illustrated in Figs. (1, 2 and 3) and the solution techniques are available in ref. [1, 2 and 3] respectively. For these configurations the models in the solution were based on the following assumptions were made: The flow is modeled as a two-dimensional, laminar, incompressible and the fluid (air) was assumed Newtonian with constant properties. The pressure work and viscous dissipation terms are negligible in the energy equation.

## 4. Results and Discussions

### 4.1 Outdoor experiment on PV module

The measured data as well as that provided by the module manufacturer are presented in table (1). As seen from the table, a power value of 52.2 W was obtained at  $G_T=906 \text{ W/m}^2$  and  $T_{\text{Cell}}=52.3 \text{ }^\circ\text{C}$  while almost the same power was obtained at  $G_T=804 \text{ W/m}^2$  and  $T_{\text{Cell}}=45.2 \text{ }^\circ\text{C}$ . In addition, the module efficiency is 7.5 % at SRC while for the cell temperature of

$52.3 \text{ }^\circ\text{C}$  the efficiency was 5.77 % and increased to 6.52% when the cell temperature became  $45.2^\circ\text{C}$  instead of a decrease in the solar irradiance by  $102 \text{ W/m}^2$  for the latter case. These results clearly indicate that, the cell temperature is the prevailing parameter affecting the module efficiency more than the solar irradiance. These measured data were obtained at moderate ambient dry bulb temperature as indicated in table (1). However, it is expected that the cell temperature will be much higher in summer time in hot arid area where ambient temperature reaches  $45^\circ\text{C}$  or higher. Therefore, to avoid a sharp decrease in photovoltaic module output power or adding extra module areas to retain the power at the design value, module thermal regulation systems should be designed when it works in hot arid reclaimed areas.

Table 1: Measured parameters and data provided by the module manufacturer

$G_T$ W/m <sup>2</sup>	$T_{\text{Cell}}$ °C	$I_{\text{mp}}$ Amps	$V_{\text{mp}}$ Volts	Maximum Power W	$\eta_o$ %	$T_{\text{Ambient}}$ °C	Wind Speed m/s
Measured values							
906	52.3	3.37	15.5	52.2	5.77	21.4	1.4
804	45.2	3.31	15.8	52.3	6.52	14.4	2.3
Data provided by the module manufacturer at SRC							
1000	25	4.4	17.0	75	7.5	Not cited	

## 4.2 Calculated Results

### 4.2.1 In-Line Plate Segments Configuration

#### 4.2.1.1 Effect of the ratio ( $l_w/l$ ) on pressure drop and friction factor

The effect of the in-line plate segments spacing ratio ( $l_w/l$ ) on total pressure drop and the friction factor ( $f$ ) at different  $Re_{Dh}$  values is shown in Fig. (4). The numerical results of the pressure drop presented in Fig. (4-a) are in (Pa) and are used to estimate the flow pumping power. As seen from the figure, as the ratio ( $l_w/l$ ) increases from zero (continuous flat plate) to values ranged from 0.6 to 0.7 corresponding to  $Re_{Dh}$  values of 400 and 1000, both the pressure drop and the friction factor increase significantly. While, at ( $l_w/l$ ) ratio higher than those values there are no changes in the pressure drop nor the friction factor values. In addition, as seen from the figure, at lower  $Re_{Dh}$  values for all values of the ratio ( $l_w/l$ ), the friction factor value is high and total pressure drop is lower (characteristics of laminar flow). This is due to that the flow along the sides of plate segments is tranquil and thus the boundary layer is not much interrupted even though when the plates spacing reaches one. On the other hand, as  $Re_{Dh}$  value increases with the increase in the ratio ( $l_w/l$ ) both of the total pressure drop and friction factor are significantly changed due to the existence of the wake in the plates gap spacing promoting flow mixing with higher local pressure drop at the leading edge of the plates.

#### 4.2.4 Effect of the ratio ( $l_w/l$ ) on the pumping power

The suggested configuration requires pumping power, which will be extracted from the PV module output power. The electrical pumping power required per square meter of the module outer surface area (in actual system the area subjected to solar irradiance) could be estimated from the following equation:

$$\text{Pumping Power/ m}^2 = [(u_{in} A_{in}) \Delta p] / (A_{outer} \eta_{overall}) \text{ (W/m}^2\text{)}$$

where  $\Delta p$  is the value presented in Fig. (4-a) and  $\eta_{\text{overall}}$  is the DC fan motor overall efficiency and is assumed to be equal to 0.5. The obtained results are presented in Fig. (5). As seen from the figure at  $(l_w/l)=0$  (continuous flat plate) for all  $Re_{Dh}$  values the maximum power required is about 2.5 W/m<sup>2</sup>. As the plate was divided into segments higher heat transfer rate is obtained, and consequently, the plate average temperature decreases combined with an increase in the pumping power.

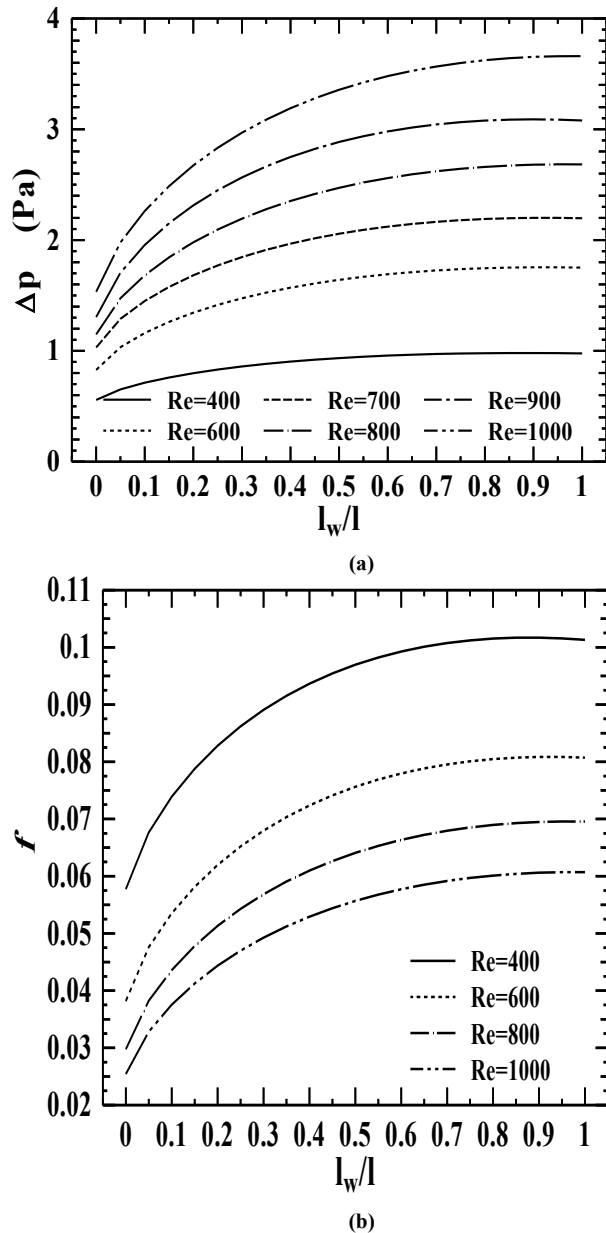


Fig. 4 Effect of plate segments spacing ratio ( $l_w/l$ ) on the total pressure drop and friction factor.

For  $Re_{Dh}=1000$  at the ratio  $(l_w/l)=0.9$  the expected required maximum electrical pumping power is about 6.2 W for each m<sup>2</sup> of the module outer area facing the sun (see Fig. (5)).

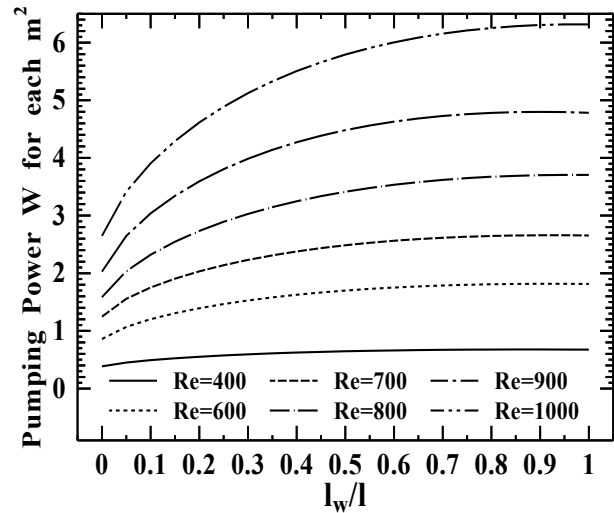


Fig. 5: Effect of plate segments spacing on the pumping power

#### 4.2.2 Oblique Plate Segments Configuration

#### 3.5 Effect of the Spacing Ratio ( $l_w/l_{pi}$ ) on the Friction Factor

The effect of the oblique plates spacing ratio ( $l_w/l_{pi}$ ) on  $f$  values at different Re values are shown in Fig. (6). It can be seen from the figure that at any angle ( $\gamma$ ) and Re values, increasing the ratio ( $l_w/l_{pi}$ ) results in a significant decrease of the friction factor. However, at low Re values and ( $l_w/l_{pi}$ ), the friction factor is very high (characteristics of laminar flow); this is due to the flow along the plates' surfaces is tranquil and the boundary layer is thick. Consequently, the viscous resistance increases. As both Re value and ratio ( $l_w/l_{pi}$ ) increase at higher values of the plates' oblique angle ( $\gamma$ ), there is no change in the friction factor. This can be explained as follows: The friction factor is estimated based on the total pressure drop through the suggested configuration, which is due to contributions from four mechanisms: viscous effects along the glass cover and back plate, losses at the plates leading and trailing edges, viscous (drag and friction) effect along the oblique plates surface and flow acceleration due to area reduction. As the plates' oblique angle increases, the flow pattern changed from channel directed flow to plates directed flow. Further increase of the ratio ( $l_w/l_{pi}$ ), the flow becomes similar to that over flat plate aligned with the channel flow. The friction due to drag for flow over a flat plate aligned with the flow is less than the friction due to drag flow in case of duct directed flow. However, as Re value increases the friction losses due to drag increase at slower rate than the skin friction. Thus, the increase in the pressure drop due to the increase in the plates' oblique angle ( $\gamma$ ) is compensated by the slower rate and divergent region formed by the plates with the channel back plate and creating deceleration flow. This leads to a partial pressure recovery. Therefore, the net pressure drop becomes almost constant for certain Re values. The reason is that an increase of friction by one pressure drop mechanism is compensated by other mechanism. Consequently, the friction factor is constant. It is found that increasing the ratio ( $l_w/l_{pi}$ ) results in a significant decrease in the friction factor until approaching a constant value depending on Re value and the plate's oblique angle ( $\gamma$ ).

### 4.2.2 Offset Plates Configuration

#### 4.2.2.1 Effect of the Offset Plate Length on the Friction Factor

The design aspect investigated is the optimum relation between one offset plate length and the hydraulic diameter of the flow channel while keeping the total length of the offset plates constant. This is obtained by assuming that, the  $N$  offset plates are positioned at  $l_1=l_3=l/3$  of Fig. (3), in accordance with the results of higher heat transfer rate from the plates. However, based on the minimum values of the friction factor ( $f$ ), figure (7) presents the variation of the friction factor ( $f$ ) along the channel with, the ratio of the channel hydraulic diameter to one offset plate length ( $D_h/l$ ), for  $Re$  values of 650 and 2550. As shown from the figure, in case of  $Re$  value of 650, the value of

( $f$ ) decreases as ( $D_h/l$ ) increases. This is true up to ( $D_h/l$ ) = 0.396, where the minimum ( $f$ ) value of 0.09997 is achieved. As the ratio ( $D_h/l$ ) increased more than 0.396, the friction factor value is increased. This can be explained as For low  $Re$  value of 650, the hydrodynamic entrance length is close to the leading edge of each offset plate. In case of the ratio ( $D_h/l$ ) is small (less number  $N$  of offset plates) the flow around each offset plate is almost developed one, which, has a relatively thick hydrodynamic boundary layer, consequently, a higher value of the friction factor. This is due to higher values of skin friction and drag forces contributions. As the ratio ( $D_h/l$ ) increases up to 0.396, (increasing number  $N$  of offset plates) excessive interruption to the flow field occurs leading to thinner hydrodynamic boundary layer, and consequently, minimum value of the friction factor.

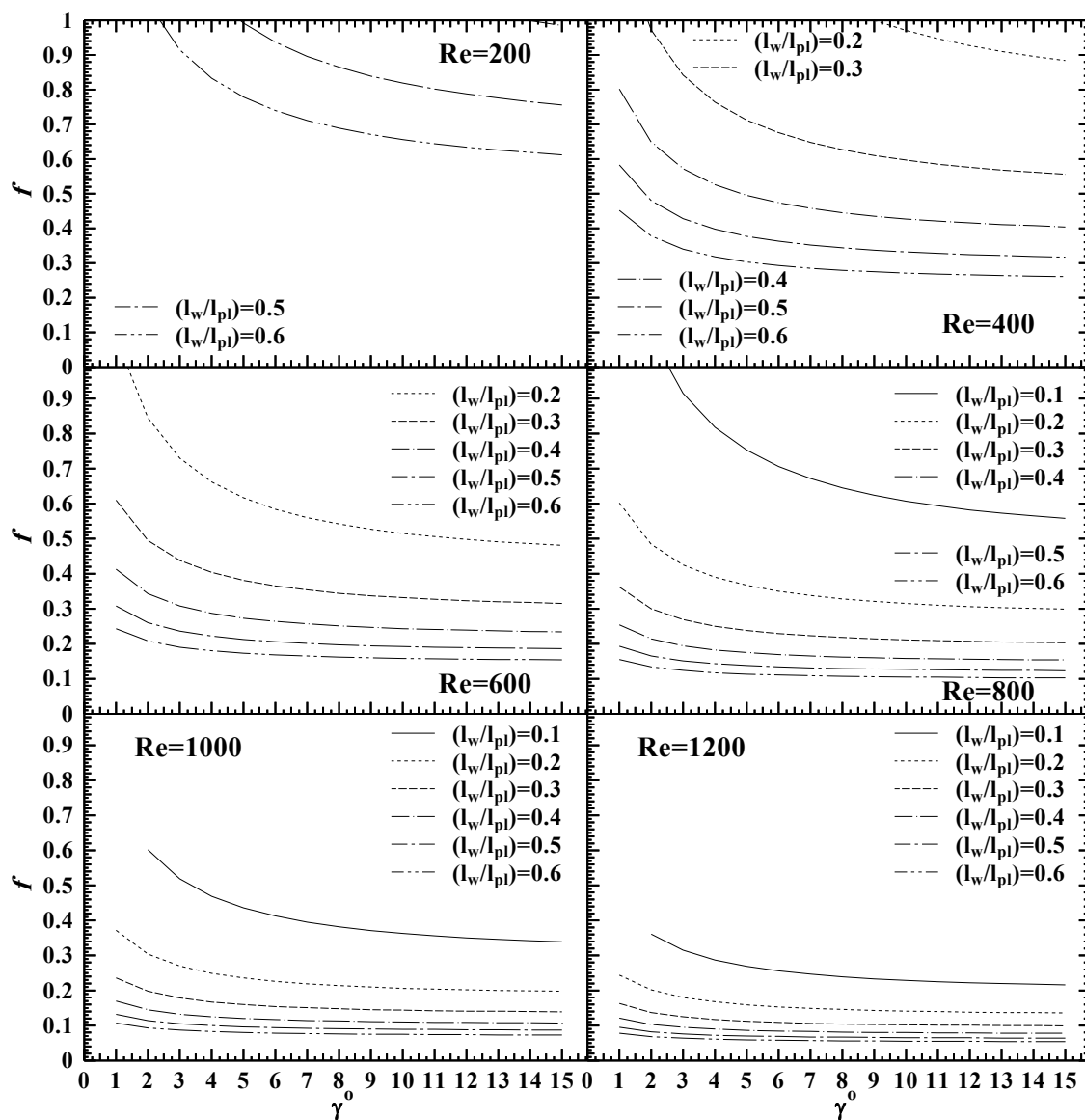


Fig. 6 Effect of plate segments spacing ratio ( $l_w/l$ ) on friction factor

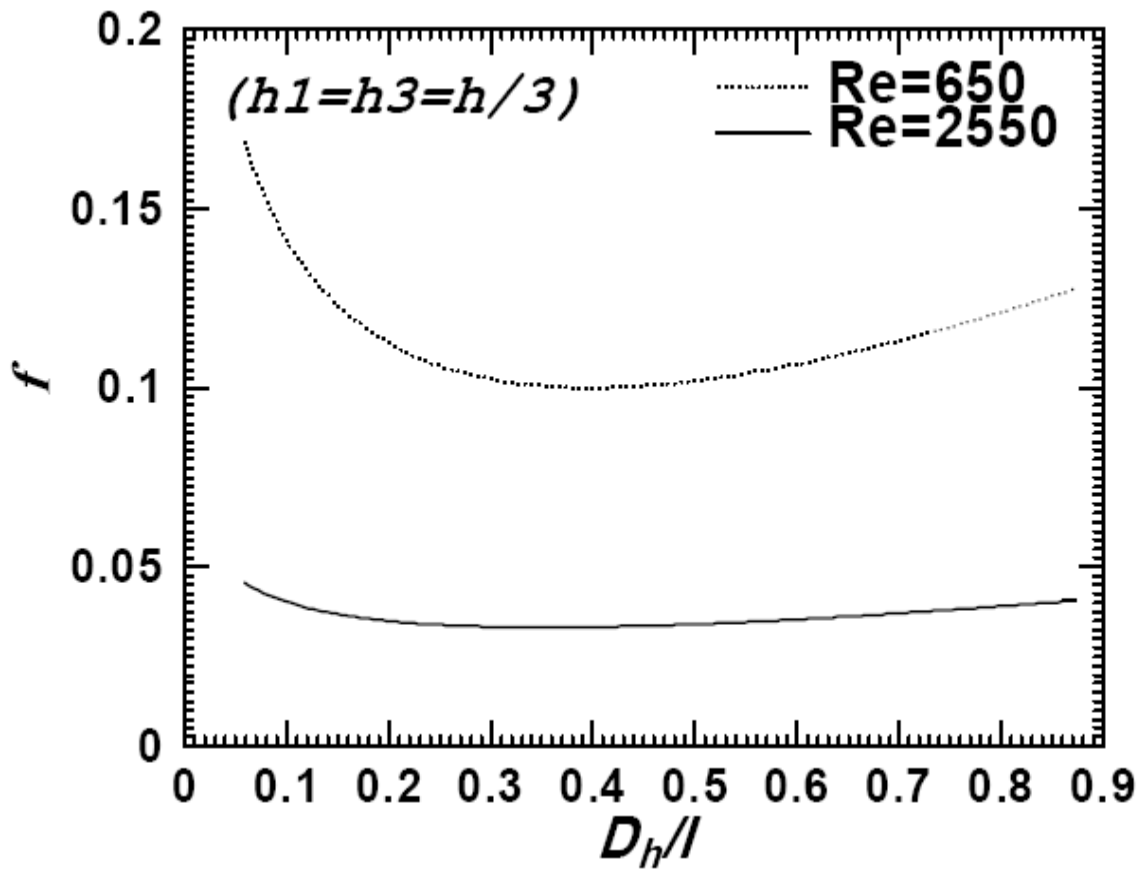


Fig. 7 Effect of the Offset Plate Length on the Friction Factor

As the ratio ( $D_h/l$ ) is increased to a value greater than 0.396, excessive interruption of the hydrodynamic boundary layer leads to more pressure drop at the leading edge of each offset plate; consequently, leads to this slight increase in friction factor again. This leads to conclusion that, based on the minimum friction factor ( $f$ ) only, and,  $Re$  value of 650 one offset plate length should be around 2.52 times of the channel hydraulic diameter. It can be seen from Fig. (7) that a low value of Reynolds number leads to a higher friction factor value. This is the characteristic of the laminar flow, where the friction factor is inversely proportional to the flow Reynolds number.

#### 4.4 Prediction of PV module characteristics using the obtained results

In appraising the obtained results, special attention is given to applying the plate segments inside channel as PV module thermal regulation system and it is important to clarify if the use of segments plate configuration does or does not increase the PV module output power and consequently the efficiency. The obtained results are presented in Fig. (8). Commercially available PV modules have module label ratings and operating parameters based on the American Society for Testing Materials (ASTM) standard reporting conditions (SRC). The

SRC are: solar irradiance  $GT = 1000 \text{ W/m}^2$ , cell temperature  $T_{\text{cell}} = 25^\circ\text{C}$ , and  $AM = 1.5$ . Thus, a typical 75 Watt PV module has 75 Watt label ratings at SRC. As seen from the figure, the PV module maximum power at SRC is 75 W (given by the manufacturer). When the module configured to plate segments and predicted average temperature of  $42^\circ\text{C}$  is used, the predicted output power is 67.9 W. For continuous flat plate with predicted average temperature of  $68^\circ\text{C}$  the predicted output power is 57.6 W. For a module without any thermal regulation system and its temperature is  $135^\circ\text{C}$ , the output predicted power is 32.3 W. The results presented in Fig. (8) indicate that, if PV modules are used without thermal regulation system, the required area should be 2.32 times the calculated PV module area at SRC, while the area became 1.1 from that at SRC when the module is configured to plate segments and cooled by air in laminar regime and this area became 1.3 from that estimated at SRC when the module is configured to continuous flat plate cooled by air in laminar regime. Thus, it is expected that, using PV modules in hot arid areas without thermal regulation leads to an increase in the total module areas ranging from 2.12 to 1.8 of that of modules using thermal regulation system producing the same power.

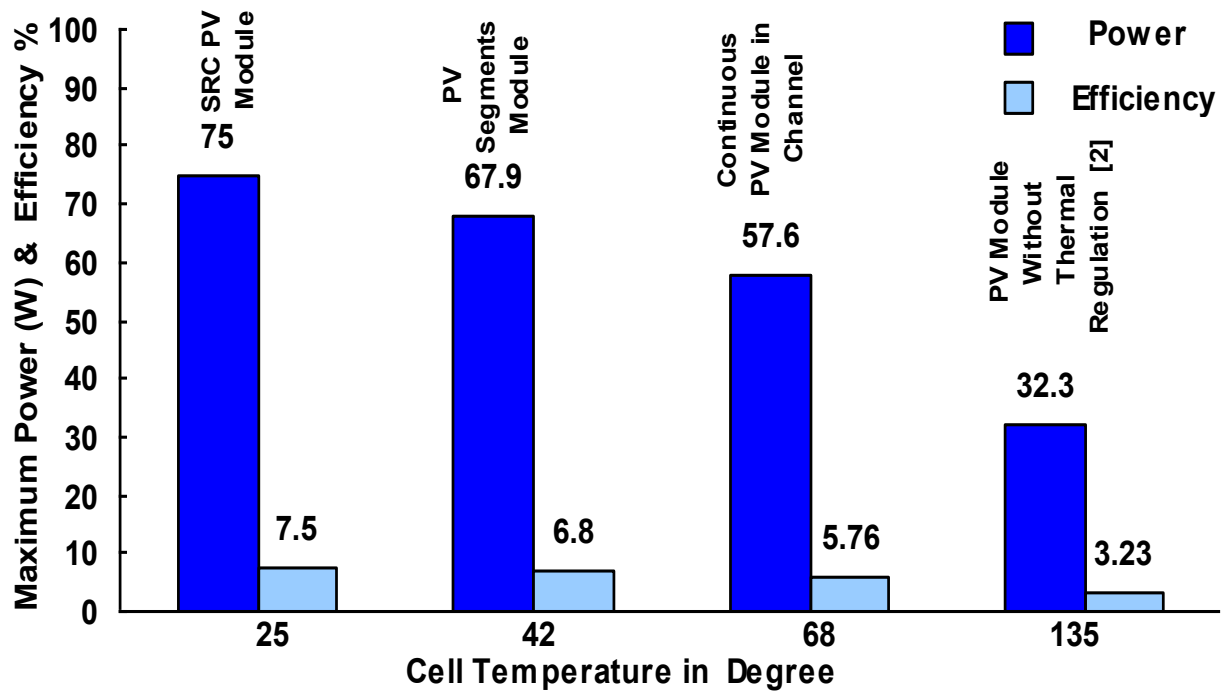


Fig. 8 Comparison of GP 75 PV crystal silicon module characteristics at different operating temperature with those at SRC

## 5. Conclusion

This study is carried out to clarify experimentally the effect of higher PV module temperature on the module output power when the module works with and without thermal regulation system. Moreover theoretical study results are used to clarify which of the three configurations, in-line, oblique and offset of the cell location inside the channel, provide higher heat transfer rate at minimum friction factor. The main findings of the present study can be summarized as follows:

- From the outdoor measurement, the results indicate that the cell temperature is the prevailing parameter affecting the module efficiencies than the solar irradiance.
- For In line plate segments configuration and  $Re_{Dh}=1000$  at the ratio  $(l_w/l_{pi})=0.9$  where highest convection heat transfer from the plate segments was predicted, the required electrical pumping power is about 6.2 W for each  $m^2$  of the surface area.
- For oblique plate segments configuration, an increase in the ratio  $(l_w/l_{pi})$  leads to a significant decrease in the friction factor value up to a constant value depending on Re value and plates oblique angle ( $\gamma$ ).
- For offset plates' configuration, at low value of Reynolds number the higher friction factor value is occurred.
- In-line plate segments configuration at certain design conditions provide the minimum friction factor, consequently, the minimum required pumping power, that will followed by higher PV module performance.
- Using PV modules in hot arid areas without thermal regulation leads to an increase in the total module areas ranging from 2.12 to 1.8 times that of module using thermal regulation system producing the same power.

## References

- [1] Ali, Ahmed Hamza H. Characteristics of flow and heat transfer for in-line plate segments inside channel used for photovoltaic modules thermal regulation. *Applied Thermal Engineering* 2005; 25(8-9): 1381-1401. <http://dx.doi.org/10.1016/j.applthermaleng.2004.06.004>
- [2] Ali, Ahmed Hamza H., Ahmed, M., Youssef, M. S., 2010, "Characteristics of Heat Transfer and Fluid Flow in a Channel with Single-Row Plates Array Oblique to Flow Direction for Photovoltaic/Thermal System", *Energy*, 2010; 35(9): 3524-3534. <http://dx.doi.org/10.1016/j.energy.2010.03.045>
- [3] Ali, Ahmed Hamza H., 2000, "Numerical Study on Design Parameters of a Channel with Staggered plate segments Heated by Radiation, Based on Maximum Forced Convection Heat Transfer Coefficient and Minimum Friction Factor", *NAFEMS Int. J. of CFD Case Studies*, 2, pp. 69-101.
- [4] Ali, Ahmed Hamza H., Hanaoka, Y., Kishinami, K., Suzuki, J., 1998, "Experimental Study of Laminar Flow Forced-Convection Heat Transfer in Air Flowing Through Staggered plate segments Heated by Radiation Heat Flux", *Int. J. comm. Heat Mass Transfer*, 25 (3), pp. 297-308.
- [5] S. Fitzpatrick (2000). A Method for Predicting PV Module and Array Performance at Other Than Standard Reporting Conditions. North Carolina Solar Center, North Carolina State University, 5P. <safitzpa@eos.ncsu.edu>